The Astrophysical Journal, 735:109 (12pp), 2011 July 10 doi:10.1088/0004-637X/735/2/109

SECULAR CHAOS AND THE PRODUCTION OF HOT JUPITERS

Yanqin Wu[1] and Yoram Lithwick[2,3]
[1] Department of Astronomy & Astrophysics, University of Toronto, Toronto, ON, Canada
[2] Canadian Institute of Theoretical Astrophysics, Toronto, ON, Canada
[3] Department of Physics & Astronomy, Northwestern University, Evanston, IL, USA
Received 2010 December 15; accepted 2011 April 16; published 2011 June 23

ABSTRACT

In a planetary system with two or more well-spaced, eccentric, inclined planets, secular interactions may lead to chaos. The innermost planet may gradually become very eccentric and/or inclined as a result of the secular degrees of freedom drifting toward equipartition of angular momentum deficit. Secular chaos is known to be responsible for the eventual destabilization of Mercury in our own solar system. Here we focus on systems with three giant planets. We characterize the secular chaos and demonstrate the criterion for it to occur, but leave a detailed understanding of secular chaos to a companion paper. After an extended period of eccentricity diffusion, the inner planet's pericenter can approach the star to within a few stellar radii. Strong tidal interactions and ensuing tidal dissipation extract orbital energy from the planet and pull it inward, creating a hot Jupiter. In contrast to other proposed channels for the production of hot Jupiters, such a scenario (which we term "secular migration") explains a range of observations: the pile-up of hot Jupiters at 3 day orbital periods, the fact that hot Jupiters are in general less massive than other radial velocity planets, that they may have misaligned inclinations with respect to stellar spin, and that they have few easily detectable companions (but may have giant companions in distant orbits). Secular migration can also explain close-in planets as low in mass as Neptune; and an aborted secular migration can explain the "warm Jupiters" at intermediate distances. In addition, the frequency of hot Jupiters formed via secular migration increases with stellar age. We further suggest that secular chaos may be responsible for the observed eccentricities of giant planets at larger distances and that these planets could exhibit significant spin–orbit misalignment.

Key words: planetary systems

Online-only material: color figures

1. INTRODUCTION

While around 10% of Sun-like stars surveyed harbor Jovian-mass planets, only ∼1% are orbited by so-called hot Jupiters with periods shortward of ∼10 days (see reviews by Marcy et al. 2005; Udry & Santos 2007). There appears to be a pile-up of hot Jupiters around 3 day orbital periods. This excess is genuine and has been confirmed by both radial velocity (RV) and transit surveys (Gaudi et al. 2005; Butler et al. 2006; Cumming et al. 2008; Fressin et al. 2007). Outward of hot Jupiters, there appears a deficit of gas giants with periods of 10–100 days (the "period valley;" Udry et al. 2003; Wittenmyer et al. 2010).

According to current theories of planet formation, hot Jupiters could not have formed in situ, given the large stellar tidal field, high gas temperature, and low disk mass to be found so close to the star. Instead, hot Jupiters most likely formed beyond a few AU and then migrated inward. Candidate migration scenarios that have been proposed include protoplanetary disks, Kozai migration by binary or planetary companions, and scattering with other planets in the system. While each of these mechanisms may have contributed to the hot Jupiter population to some degree, the question remains as to which is the dominant one. The dominant mechanism has to explain a variety of observed correlations. In Section 2, we review some of these correlations and provide a critical assessment of the above three mechanisms.

In this work, we propose a fourth channel for producing hot Jupiters, namely, planet migration by secular chaos. Secular chaos may arise in planetary systems that are well spaced and are dominated by long-range secular interactions. A system of two non-coplanar planets can be chaotic, but only if their eccentricities and inclinations are of order unity (Libert & Henrard 2005; Migaszewski & Goździewski 2009; Naoz et al. 2011). So, in this paper we focus on systems with three planets. The criterion for secular chaos is less stringent, and the character of secular chaos is more diffusive, differing from that of the two-planet case. This diffusive type of secular chaos promotes energy equipartition between different secular degrees of freedom. The physics behind secular chaos is analyzed in detail in a companion paper (Lithwick & Wu 2011), where we show that Mercury, the innermost planet in our solar system, experiences a similar type of secular chaos. Mercury may consequently be removed from the solar system (Laskar 2008; Batygin & Laughlin 2008; Laskar & Gastineau 2009).

Secular chaos tends to remove angular momentum in the innermost planet gradually, causing its pericenter to approach the star. Tidal dissipation may then remove orbital energy from this planet, turning it into a hot Jupiter. Hot Saturns or hot Neptunes may also be produced similarly. Such a migration mechanism, which we term "secular migration," can reproduce a range of observations. It also predicts that in systems with hot planets, there are other giant planets roaming at larger distances.

2. HOT JUPITERS: OBSERVATIONS AND THEORIES

2.1. Observations

There is a sharp inner cutoff to the 3 day pile-up of hot Jupiters. They appear to avoid the region inward of *twice* the Roche radius (Ford & Rasio 2006), where the Roche radius is the distance within which a planet would be tidally shredded. New data spanning two orders of magnitude in planetary masses (and including planet radius measurements) have strengthened this claim. There are only five known exceptions lying inward

of twice the Roche radius, and the rest mostly lie between twice and four times the Roche radius.

Hot Jupiters appear to be less massive than more distant planets (Pätzold & Rauer 2002; Zucker & Mazeh 2002). For planets discovered with the RV method, close-in planets have projected masses ($M \sin i$) less than twice Jupiter's mass, excluding planets in multiple star systems. But numerous planets farther out have $M \sin i > 2\,M_J$ (Udry & Santos 2007, Figure 5).

Many hot Jupiters have orbits that are misaligned with the spin of their host stars. The angle between the orbit normal of a transiting planet and the spin axis of its host star (the stellar obliquity) can be probed with the Rossiter–McLaughlin (R-M) effect (e.g., Winn et al. 2005). Planets were presumably born in a disk aligned with the stellar spin. Therefore, measurements of the present stellar obliquity provide a stringent constraint on the migration scenario. Analysis of the first 11 systems with R-M measurements found that the majority were consistent with perfect alignment, while a small minority were highly misaligned (Fabrycky & Winn 2009). However, later analysis that included more systems (26 in total) found that most are misaligned, and many of these are even in retrograde orbits (Triaud et al. 2010). The reason for this discrepancy is currently unclear.

Hot Jupiters also tend to have few companions, at least out to a few AU. From RV surveys, ∼30% of planets are in multiple planet systems (including ones with RV trends; Butler et al. 2006), while only five hot Jupiters are (HD 187123b, HIP 14810b, ups Andb, HAT-P-13b, and HD 217107b; Wright et al. 2009; Hebrard et al. 2010a); i.e., fewer than 10% of hot Jupiters are known to have companions within a couple AU. This relative deficit also shows up in the transit sample, where most attempts at detecting transit timing variations caused by close companions (Holman & Murray 2005; Agol et al. 2005) have been unsuccessful (e.g., Rabus et al. 2009; Csizmadia et al. 2010; Hrudková et al. 2010), except for, perhaps, Maciejewski et al. (2010, 2011) and Fukui et al. (2011).

2.2. Migration Theories

The successful migration scenario has to explain these and other observed correlations. There are two categories of migration scenarios. One is for the planet to migrate within a gaseous disk (disk migration). The other is to generate high eccentricity in the planet, bringing it sufficiently close to the star that tidal dissipation circularizes and shrinks its orbit into that of a hot Jupiter. The latter category includes Kozai migration, planet–planet scattering, as well as the secular chaos that we propose in this work.

We first examine disk migration, a theory that pre-dated the discovery of hot Jupiters (Lin & Papaloizou 1986). It asserts that the viscous protoplanetary disk carries the planet inward (Chambers 2009; Rice et al. 2008). The presence of mean-motion resonance (MMR) pairs among observed planets seems to support this scenario. However, to produce the observed pile-up of hot Jupiters at around 3 day orbital periods, the inward migration has to be halted. As discussed by Lin et al. (1996), this could be achieved if the disks are truncated by the stellar magnetosphere at a radius that corresponds to twice the planet's orbital period. Disks are likely truncated at the corotation radius, where the orbital period of the disk material equals the spin period of the star. The observed distribution of rotation periods of pre-main-sequence stars appears to be bimodal (Herbst & Mundt 2005) with the location of the long-period peaks varying from 4 to 8 days for different clusters. This could be consistent with the period distribution of hot Jupiters. It is also plausible that hot Jupiters that have thus migrated would tend to be lower in mass, although that has yet to be shown. A difficulty with this scenario is that it should produce planets whose orbit normals are aligned with the stellar spin axis (for an opposing view, however, see Lai et al. 2011). In addition, it remains to be argued why hot Jupiters rarely have close companions (within a few AU) if they migrated inward due to powerful disks. There is no natural explanation in this scenario for the avoidance of twice the Roche radius.

We now turn our attention to planet–planet scattering. First proposed by Rasio & Ford (1996), it asserts that close encounters between planets can induce extreme eccentricity in one of the planets (Ford et al. 2001; Papaloizou & Terquem 2001; Ford & Rasio 2008), which may then be tidally circularized to form a hot Jupiter. Such a theory reproduces the observed eccentricity distribution of (non-hot) extra-solar planets that have $e \gtrsim 0.2$ (Chatterjee et al. 2008; Jurić & Tremaine 2008), as well as the observed close-packed nature of pairs (Raymond et al. 2009). It may also account for the high inclinations of hot Jupiters. However, it is unclear if the initial condition of a compact and highly unstable planetary system as required by this theory is applicable to planets emerging from a gaseous disk (Matsumura et al. 2010). Also, Chatterjee et al. (2008) find that the inner planets tend to be the most massive ones, contrary to the observed correlations. Furthermore, since scatterings are sudden, it is difficult for tides, a slow process, to halt scattered planets (Nagasawa et al. 2008). This theory also predicts readily detectable outer planets that are responsible for scattering and producing the observed hot Jupiters. They are, however, not observed.

Lastly, we comment on Kozai migration. First proposed by Wu & Murray (2003), it asserts that a highly inclined companion star can induce Kozai oscillations (Kozai 1962; Eggleton & Kiseleva-Eggleton 2001) in the planet, gradually exciting the planet to a high enough eccentricity that it approaches the central star, whereupon tidal dissipation circularizes it into a hot Jupiter. While it succeeds in producing hot Jupiters that are highly inclined with respect to stellar spin, including ones that are retrograde in projection (Triaud et al. 2010), and is likely responsible in a number of specific cases (such as HD 80606b Naef et al. 2001; Laughlin et al. 2009; Pont et al. 2009; Winn et al. 2009; Hebrard et al. 2010b), it does not preferentially yield low-mass hot Jupiters[4] and its effectiveness may be hampered by the presence of other planets in the system (Wu & Murray 2003). Furthermore, population studies establish that only ∼10% of hot Jupiters can be explained by Kozai migration due to binary companions (Wu et al. 2007; Fabrycky & Tremaine 2007).

Mechanisms that rely on eccentricity excitation, such as Kozai migration or planet-planet scattering, naturally produce hot Jupiters that tend to avoid the region inside twice the Roche radius (Ford & Rasio 2006). However, only Kozai migration can naturally explain the 3 day pile-up, as the eccentricity rise in this case is gradual and planets are accumulated at the right location. The secular chaos mechanism described in this paper also leads to gradual eccentricity excitation and can therefore inherit much of the success of the Kozai mechanism.

The noteworthy simulations of Nagasawa et al. (2008) combine planet scattering with Kozai oscillations. Starting from very

[4] Kozai migration can readily make massive planets migrate inward and perhaps can account for the presence of massive hot Jupiters found in binary systems (Zucker & Mazeh 2002).

Table 1
Initial Conditions for the Example System

Pl.	Mass (M_J)	a (AU)	e	Inc. (deg)	ω (deg)	Ω (deg)
1	0.5	1	0.066	4.5	π	0
2	1.0	6	0.188	19.9	0.38π	π
3	1.5	16	0.334	7.9	π	0

compact systems of three equal-mass planets, their planets frequently scatter one another onto highly inclined orbits, which in some cases trigger Kozai oscillations. Their particular setup yields hot Jupiters ∼30% of the time, with orbital inclinations that are roughly isotropic. The production of hot Jupiters by inter-planet Kozai oscillations has also been studied in Naoz et al. (2011). Such a mechanism appears promising if eccentricities and inclinations can reach order-unity values.

2.3. Secular Interactions

Secular interactions are a simplified version of interplanetary interactions, where one can account for the forces between two planets by calculating the torque between two mass wires. The latter are made by spreading the mass of a planet along its orbit, weighted by the amount of time it spends at that segment. This describes the dynamics adequately as long as the planets have no close encounters and do not lie near MMRs. Secular interactions allow planets to exchange angular momentum but not energy. So, planets' semimajor axes are unchanged. The long-term evolution of the inner solar system, for instance, is primarily secular in nature (Laskar 1989).

Under certain circumstances, secular interactions can gradually raise the eccentricity of the inner planet to near unity, even when the initial eccentricity are as low as that expected of planets emerging out of dissipative gaseous protoplanetary disks. This is the work of chaos.

When planet eccentricities and inclinations are small, secular dynamics is fully described by a linear summation of secular eigenmodes that are independently oscillating, abiding by the so-called Laplace–Lagrange theory (see, e.g., Murray & Dermott 2000). The multi-periodic variations in the eccentricity of the Earth are largely caused by the interference between the eigenmodes. These have been claimed to drive climate changes (Milankovitch 1941).

When eccentricities and inclinations rise, linear eigenmodes no longer describe the dynamics adequately. Nonlinear effects can occur. One example is the appearance of nonlinear secular resonances, including new fixed points and separatrices that are not present in the linear system (Michtchenko & Malhotra 2004; Michtchenko et al. 2006; Migaszewski & Goździewski 2009). A second is the chaotic motion associated with the overlap of neighboring resonances (Sidlichovsky 1990; Michtchenko et al. 2006; Lithwick & Wu 2011).

For a system of two planets, strong nonlinearity and chaos requires eccentricities and/or inclinations of order unity. If the two planets are coplanar, energy and angular momentum conservation constrain the motion to be regular and quasi-periodic. But if the planets are sufficiently inclined, the Kozai resonance can be triggered, leading to instability and/or chaos. This requires mutual inclinations $\gtrsim 40^\circ$ if the initial eccentricities are very large and $\gg 40^\circ$ for more modest eccentricities (Michtchenko et al. 2006; Naoz et al. 2011). For instance, for the inner two planets listed in Table 1 to interact to produce $e_1 > 0.98$, a mutual inclination of $>85^\circ$ is necessary.

For a system of three or more planets, however, the threshold for chaos is much reduced. Moreover, the nature of the secular chaos is different. In the two-planet case, chaotic systems are quickly unstable on the secular timescale, ∼10 Myr for typical parameters (Michtchenko et al. 2006; Naoz et al. 2011). By contrast, in the multi-planet case a multitude of resonances can overlap. This leads to a gentler type of chaos, with the orbital elements gradually diffusing over many secular times, while the values of the eccentricities and inclinations remain modest. An example of the latter type of behavior is the inner solar system, where chaos is prevalent even at eccentricity/inclination levels of a few percent, and the timescale of the evolution is ≫Gyr (Laskar 1989; Lithwick & Wu 2011).

In the following, we investigate a planetary system with three mildly eccentric and inclined planets to demonstrate the appearance of this new type of secular chaos—new, that is, in the context of extra-solar planetary systems.

3. SECULAR CHAOS: A WORKED EXAMPLE

3.1. Numerical Example

Initial conditions. Parameters for the example system we investigate are listed in Table 1. The inclinations are measured relative to the system's invariable plane.

For the semimajor axes, we space the planets sufficiently far apart and away from any major MMRs (orbital period ratios are 1:14.7:64). The choice for the masses is somewhat arbitrary, except for our choice that the innermost planet be the least massive, which facilitates its excitation.

The somewhat odd-looking choices for the other orbital elements place most of the secular energy (i.e., angular momentum deficit) in the outer planets, or more specifically in the secular eigenmodes associated with those planets (more detail in Section 4). We find that the occurrence of secular chaos is not particularly sensitive to our choices for these values, as long as the system has sufficient amount of angular momentum deficit (AMD; Section 4).

Numerics. This simulation was performed using the SWIFT symplectic integrator (Levison & Duncan 1994), supplemented with routines that model tidal dissipation in the planet and in the star, precessions due to general relativistic (GR) effects, and precessions due to rotational and tidal bulges on both the inner planet and the star. Details are presented in the Appendix. These effects are essential for determining the final positions of the hot Jupiters.

Numerical precision at extremely high eccentricities is of concern. So, we adopt a time step that is 1/100 of the inner planet's orbital period (1 yr) for most of the integration, but switch it to a value 100 times shorter whenever the periastron of the inner planet reaches inward of 0.1 AU from the star. We find that such a change of time step, even though it breaks the time symmetry of the symplectic integrator, is required to maintain satisfactory energy and angular momentum conservation. The fractional energy error, integrated over an episode of extremely high eccentricities (which typically lasts $\sim 10^4$ yr), remains below 10^{-4} as long as $e_1 < 0.98$, sufficiently small for our problem at hand.

The angular momentum error is much smaller.

Results (*Figures 1 and 2*). Our fiducial three-planet system is chaotic due to secular interactions. The random exchanges of angular momentum (but not energy) among planets induce large fluctuations in their eccentricities and inclinations. The orbit of the inner planet, starting from initial values of $e_1 = 0.07$

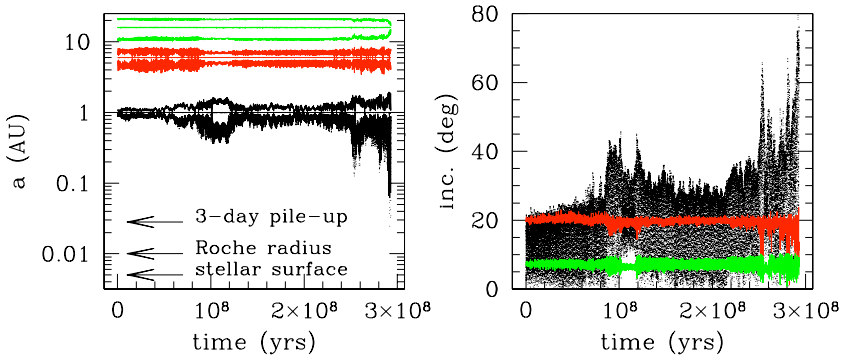

Figure 1. Formation of a hot Jupiter in our fiducial system (SWIFT integration with tides and GR). Left: radial excursions of the three planets (semimajor axis, periapse, and apoapse) are shown as functions of time, with the various radii relevant for hot Jupiters marked by arrows; right: planet inclinations measured relative to the system's invariable plane. All planets initially have mildly eccentric and inclined orbits, but over a period of 300 Myr, so much of the angular momentum in the innermost planet can be removed that its eccentricity and inclination can diffusively reach order-unity values. Planet interactions leave all semimajor axes unchanged, a tell-tale sign that secular interactions dominate the dynamics. At ∼300 Myr, the pericenter of the inner planet reaches inward of a few stellar radii and tidal interaction with the central star kicks in (details in Figure 2). Precessions by general relativity, by tidal and rotational quadruples, as well as tidal dissipation, prevent the pericenter from reaching inward of the Roche radius. As a result, the final hot Jupiter has a period of ∼3 days.

(A color version of this figure is available in the online journal.)

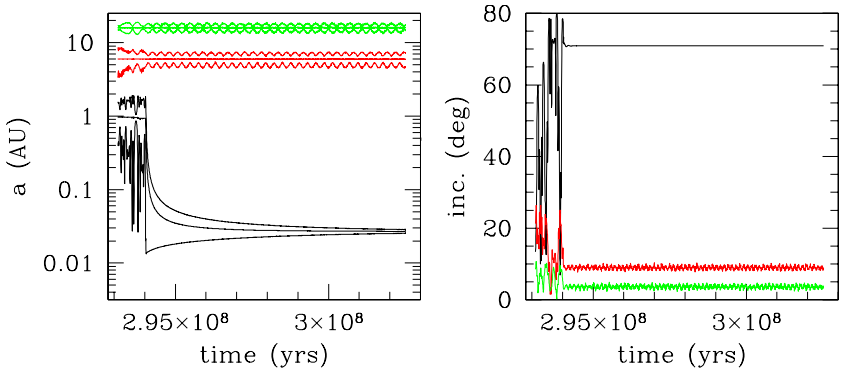

Figure 2. Same as that in Figure 1 but expanding the time axis around 300 Myr to highlight the process of tidal circularization. Secular chaos raises the inner planet's eccentricity diffusively to a maximum value of 0.985, and decreases its periapse to $a_1 * (1 - e_1) \sim 0.015$ AU—as determined by a balance between secular forcing and close-range forces. When this occurs (at time 294 Myr), tidal dissipation in the inner planet removes orbital energy while conserving orbital angular momentum. This brings the planet from an initial orbit of $a_1 = 1$ AU to an orbit of $a_1 \approx (1\text{–}0.985^2) \times 1$ AU ~ 0.027 AU. It is then dynamically decoupled from the outer two planets. Since the total angular momentum deficit (AMD) in the system is absorbed by the inner planet (and subsequently removed by tidal dissipation), the outer two planets lose AMD, and hence become more circular and coplanar after the hot Jupiter has formed. The inclination of the final inner orbit relative to the invariable plane is ∼70° (right panel). The evolution is highly chaotic, and a slight modification of the initial conditions changes the evolution dramatically (see Figure 5).

(A color version of this figure is available in the online journal.)

and $i_1 = 4°$, by 300 Myr has diffused to $e_1 = 0.985$ and $i_1 = 70°$. It has lost almost all of its initial angular momentum to the outer planets; equivalently, it has stolen some of the outer planets' AMD.

We find that the orbital elements of the inner planet undergo a random walk to most of the phase space allowed by the total energy and angular momentum. However, there are a few forbidden regions. The most important one is the region of very high eccentricity. The inner planet prudently avoids the Roche zone. This occurs because when the pericenter of the inner planet ($a_1(1 - e_1)$) approaches the star to within a few stellar radii, finite-size effects (quadrupole precessions associated with the tidal and rotational deformations on the planet and the star, respectively), as well as general relativity, combine to suppress the secular forcing. Were it not for these additional precessional effects, the inner planet could be driven to tidal disruption and merger with the central star. But as it is, the inner planet stays within $e_1 \leqslant 0.985$ or $a_1(1 - e_1) \geqslant 0.017$ AU in our system. We explain this in the following.

Due to secular interactions with other planets, the inner planet's longitude of pericenter precesses at the rate

$$\frac{d\varpi}{dt}|_{\rm sec} \approx \frac{M_p}{M_*}\alpha^3 n_1, \qquad (1)$$

where M_p is the mass of the perturbing planet and $\alpha = a_1/a_p$ is the ratio of the semimajor axes. This is disturbed by the prograde precession induced by the close-range forces. Comparing the orbit-averaged rates (Sterne 1939; Shakura 1985; Wu & Goldreich 2002) for the four types of quadrupole precessions and for GR, for the following parameters: a Jupiter-like planet with a spin period of 3 days, orbiting at $a = 1$ AU around a Sun-like star that is spinning with a period of 10 days, we conclude that the tidal bulge raised by the star on the planet dominates the precession at high eccentricities with the GR effect following not far behind. The orbit-averaged precession due to the tidal quadrupole on the planet is

$$\frac{d\varpi}{dt}|_{\rm tide} = 7.5 k_2 n_1 \frac{\left(1 + 3e_1^2/2 + e_1^4/8\right)}{\left(1 - e_1^2\right)^5} \frac{M_*}{M_1}\left(\frac{R_1}{a_1}\right)^5, \qquad (2)$$

where k_2 is the tidal Love number of the planet, taken to be $k_2 = 0.26$, and n_1, e_1, a_1, and R_1 are the planet's mean-motion, eccentricity, semimajor axis, and radius, respectively. Since this rate rises steeply as the planet approaches the star, we expect that the secular driving is arrested when the planet's pericenter reaches inward of

$$a_1(1-e_1) \sim 0.015\,\mathrm{AU}\left(\frac{M_1}{M_J}\right)^{-1/5}\left(\frac{M_p}{M_J}\right)^{-1/5}\left(\frac{M_*}{M_\odot}\right)^{2/5} \times \left(\frac{\alpha}{1/6}\right)^{-3/5}\left(\frac{R_1}{R_J}\right). \quad (3)$$

This stalling radius is independent of the planet's initial position (a_1), and weakly dependent on the planetary and stellar masses, as well as on the planet spacing in the system (i.e., the value of α). It does, however, scale with the size of the planet linearly. Since Jupiter-like planets have a fairly uniform radius, the stalling distance spans a narrow range for a wide range of system parameters.

When the orbit of such a planet is tidally circularized, the final semimajor axis is moved to twice its stalling radius, $a_1' \simeq 2 \times 0.015 \sim 0.03$ AU.[5] This explains why the hot Jupiters are piled up at the distance they are observed today (Figure 2).

The strength of the *dissipative* tide can also have an effect on the final orbit. Even if the above precessional effects are absent, the progression of the inner planet toward the star will be halted by the dissipative tide, albeit at a somewhat closer distance.

4. ANALYSIS

For secularly interacting systems, there is an important conserved quantity, the AMD (e.g., Laskar 1997)

$$\mathrm{AMD} \equiv \sum_{k=1}^{N} \Lambda_k \left(1 - \sqrt{1-e_k^2}\cos i_k\right), \quad (4)$$

where N is the number of planets, Λ_k the circular angular momentum of planet k, $\Lambda_k = \frac{m_k M_\odot}{m_k+M_\odot}\sqrt{G(M_\odot+m_k)a_k}$, and i_k is its inclination relative to the invariable plane (normal to the total angular momentum). Since the total angular momentum is conserved, and secular interactions do not modify the orbital energies (a_k constant), the AMD is conserved during secular interactions. For circular, coplanar systems, the AMD is zero, and the AMD increases with increasing e's and i's.

Here, we analyze our numerical results to illustrate the condition for hot Jupiter formation. We find that a sufficient amount of AMD is required. First, the value of AMD limits the maximum eccentricity and inclination an individual planet can attain (Section 4.1). Second, only when AMD is large enough can it be shared among different secular eigenmodes (equipartition), ultimately driving the inner planet to extreme orbits. We call this sharing process "secular chaos." We illustrate the deep analogy between AMD and kinetic energy in a thermodynamical system in Section 4.2, and analyze the diffusive and chaotic nature of the energy sharing process in Sections 4.3 and 4.4. We also briefly look at the issue of AMD generation by MMRs in the system (Section 4.5).

[5] Angular momentum ($\propto \sqrt{a(1-e^2)}$) is roughly conserved during tidal dissipation. So, the post-circularized a_1' is related to the pre-circularized a_1 via $a_1' = a_1(1-e_1^2) \simeq 2a_1(1-e_1)$.

4.1. Maximum Eccentricity and Inclination

To be propelled into the hot Jupiter status, the inner planet has to reach so close to the star that tidal dissipation operates. Let this be roughly $a_1(1-e_1) \leqslant 0.05$ AU. If all AMD can be transferred to the inner planet, this condition translates into

$$\mathrm{AMD} \geqslant \Lambda_1\left[1 - \left(\frac{a_1}{0.1\,\mathrm{AU}}\right)^{-1/2}\cos i_1\right]. \quad (5)$$

So, a planet that is closer to the star and lower in mass needs less AMD to become a hot Jupiter. From now on we measure AMD in units of the circular angular momentum of the inner planet ($\Lambda_1 = 1$). The above condition translates into

$$\mathrm{AMD} \geqslant 1 - 0.3\cos i_1 \quad (6)$$

for $a_1 = 1$ AU. So, to produce a coplanar hot Jupiter ($i_1 = 0$), AMD > 0.7, while a retrograde hot Jupiter would require AMD > 1.0. Fortunately, this is not difficult to satisfy. Our example system has AMD $= 1.17$ even though the eccentricities are modest—comparable to or lower than those in observed systems. The outer planets can carry a great deal of AMD even at low values of eccentricity/inclination. Retrograde hot Jupiters can potentially be produced.

4.2. AMD and Kinetic Energy

The AMD is for a secularly interacting system what kinetic energy (or temperature) is for a thermodynamical system. This analogy runs deep as we shall show here.

We introduce the complex Poincaré variables z_k and ζ_k (see, e.g., Laskar 1997; Murray & Dermott 2000),

$$z_k = \sqrt{2}\sqrt{1-\sqrt{1-e_k^2}}\exp(i\varpi_k),$$
$$\zeta_k = \sqrt{2}\sqrt{\sqrt{1-e_k^2}(1-\cos i_k)}\exp(i\Omega_k), \quad (7)$$

where ϖ_k is the longitude of periapse and Ω_k is the longitude of the ascending node. At low eccentricities and inclinations, $z_k \approx e_k\exp(i\varpi_k)$ and $\zeta_k \approx i_k\exp(i\Omega_k)$. The AMD may then be recast as (Laskar 1997)

$$\mathrm{AMD} = \sum_{k=1}^{N}\frac{\Lambda_k}{2}(|z_k|^2 + |\zeta_k|^2). \quad (8)$$

The resemblance of AMD to kinetic energy becomes obvious in this form: while the "inertial mass" for each planet corresponds to its circular angular momentum Λ_k, the (z_k, ζ_k) pair corresponds to its "velocity."

When AMD is zero, the system will remain coplanar and circular and stable forever. At low AMD, secular interactions lead to periodic exchanges of angular momentum between planets. This, however, is not related to the equipartition process. The dynamics can be decomposed into that of linear secular eigenmodes and the periodic variations in orbital elements are caused by the interference between these modes (the so-called Laplace–Lagrange theory). Each linear mode oscillates at its characteristic eigenfrequency with constant amplitude and phase. Let the eigenvectors be $\tilde{z}_{k\alpha}$ and $\tilde{\zeta}_{k\alpha}$. They are orthonormal after each component is pre-multiplied by $\sqrt{\Lambda_k/2}$, i.e., $\sum_k \frac{\Lambda_k}{2}\tilde{z}_{k\alpha}\tilde{z}_{k\beta} = \sum_k \frac{\Lambda_k}{2}\tilde{\zeta}_{k\alpha}\tilde{\zeta}_{k\beta} = \delta_{\alpha\beta}$, where $\delta_{\alpha\beta}$ is the

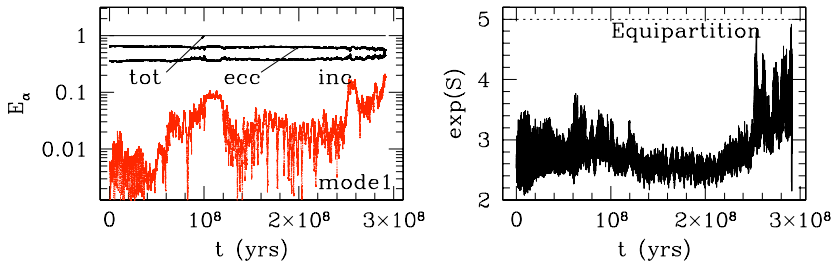

Figure 3. Diffusive behavior for the system in Figure 1, demonstrated using eigenmode energies (really, AMDs) and spectral entropy. The curves in the left panel are, from top to bottom, total AMD, AMD in eccentricity modes, AMD in inclination modes, and AMD in the eccentricity mode associated with the inner planet, all plotted as their ratio to the total AMD (which is conserved to better than a percent before tidal dissipation sets in). For clarity, the last three are plotted as running overages (over 2×10^4 yr). The first eccentricity mode gains AMD from other modes, and there is AMD exchange between eccentricity and inclination modes. The right-hand panel shows the exponential of the spectral entropy, $\exp(S)$, as expressed in Equation (10). The process of AMD equipartition raises $\exp(S)$ from 2 (two modes dominating the AMD) to ∼5 (all modes share comparable AMD, marked by the dotted curve). When tidal dissipation sets in, the total AMD decreases, leading to a drop in the entropy. If we turn off the dissipation and integrate the system further, we observe that the spectral entropy fluctuates, but it seldom departs from the equipartition value for an extended period.

(A color version of this figure is available in the online journal.)

Kronecker delta; the overall phase of each eigenvector is chosen so that all components are real. Projecting the complex orbital elements onto these eigenvectors, $z_k = \sum_{\alpha=1}^{N} a_\alpha \tilde{z}_{k\alpha}$, $\zeta_k = \sum_{\alpha=N+1}^{2N-1} a_\alpha \tilde{\zeta}_{k\alpha}$,[6] we can re-express AMD as

$$\mathrm{AMD} = \sum_{\alpha=1}^{2N-1} |a_\alpha|^2. \tag{9}$$

Each eigenmode resembles one degree of freedom in a thermodynamical system, and the AMD resembles the total energy. In the linear solution, if one mode is initially assigned all the AMD, it will retain it forever. As a result, each planetary orbit moves within a certain bound as given by the initial condition.

As AMD rises, energy transfer (or really, AMD transfer) becomes non-periodic and chaotic. Orbital elements are allowed to wander as in a random-walk diffusion. This may ultimately lead to AMD equipartition between different secular modes (different degrees of freedom in the system), as well as approximate AMD equipartition between different planets.[7] The least massive or the closest planet has the smallest inertia. AMD equipartition implies that such a planet can reach very high eccentricity and/or inclination, providing the condition for hot Jupiter formation.

4.3. Diffusion of AMD Observed

Diffusion of energy in a weakly nonlinear system is an extensively studied subject, starting from the famous Fermi–Pasta–Ulam problem (E. Fermi et al. 1955, unpublished). In the following, we present evidence for AMD diffusion in our example system and illustrate the criterion for AMD diffusion.

One line of evidence comes from the amplitudes of the secular eigenmodes.[8] The initial conditions chosen in Table 1 correspond to deliberately depositing almost all AMD into the secular modes associated with the outer planets and little in the eccentricity mode associated with the inner planet. There are three advantages to this. First, AMD transfer between modes occurs on secular or longer timescales. So, for the first tens of millions of years, all three planets have small e's and i's, as appropriate for planets emerging from a protoplanetary disk. Second, by initializing the inner eccentricity mode with low amplitude, we are farthest away from our preferred end state, when this mode acquires enough AMD to place the inner planet on a $e \sim 1$ orbit and a tidal encounter with the star. Third, by concentrating AMD into only a few modes, we can best observe the approach toward equipartition.

Table 2
Frequencies and Amplitudes (Initial and Final) of the Five Linear Secular Eigenmodes

Mode	Frequency	Amplitude ($\lvert a_\alpha \rvert$)	
	(arcsec yr^{-1})	$t = 0$	2.9×10^8 yr
e1	4.83	0.03	0.63
e2	8.30	0.31	0.21
e3	2.04	0.83	0.51
i1	−4.61	0.14	0.24
i2	−10.57	0.62	0.64

Table 2 and Figure 3 show that after 294 Myr of evolution (right before tidal dissipation sets in), the AMD of mode 1 has grown diffusively by a factor of $\sim 20^2 \sim 400$, while the total AMD $= \sum_\alpha |a_\alpha|^2$ remains constant. The normalization of $|a_\alpha|$ in Table 2 is such that the circular angular momentum for the innermost planet (at 1 AU) has the numerical value of one. AMD equipartition is reached in $\sim 2.5 \times 10^8$ yr.

A second way to quantify diffusion is by tracing the "spectral entropy" (Livi et al. 1985; Goedde et al. 1992)

$$S \equiv -\sum_{\alpha=1}^{2N-1} E_\alpha \ln E_\alpha, \tag{10}$$

where $E_\alpha = |a_\alpha|^2 / \sum_\alpha |a_\alpha|^2$ is the fractional energy (AMD) in mode α. This entropy increases from its minimum value of 0 (when one mode has all the AMD) to the maximum value of $\ln N_{\mathrm{mod}} = \ln(2N_{\mathrm{pl}} - 1) = \ln 5$ as the system diffuses toward energy equipartition. Spectral entropy is analogous to entropy in a thermodynamical system.

Figure 3 shows that for our example system, AMD is gradually shared among different eccentricity and inclination

[6] There is a trivial inclination mode with zero frequency, which corresponds to the overall tilt of the reference plane. Here, we take the reference plane to be the invariable plane, so the amplitude of this mode is zero.

[7] Equipartition of AMD among planets is only approximately correct. As an example, the four terrestrial planets in the solar system have similar AMD today. They have likely undergone extensive chaotic diffusion in the past.

[8] Here, we decompose using the linear eigenvectors even though they are invalid at large amplitudes. A more rigorous approach may be to decompose using nonlinear eigenvectors, as is done in Laskar (2008). But our approach suffices for the purpose of illustrating AMD diffusion.

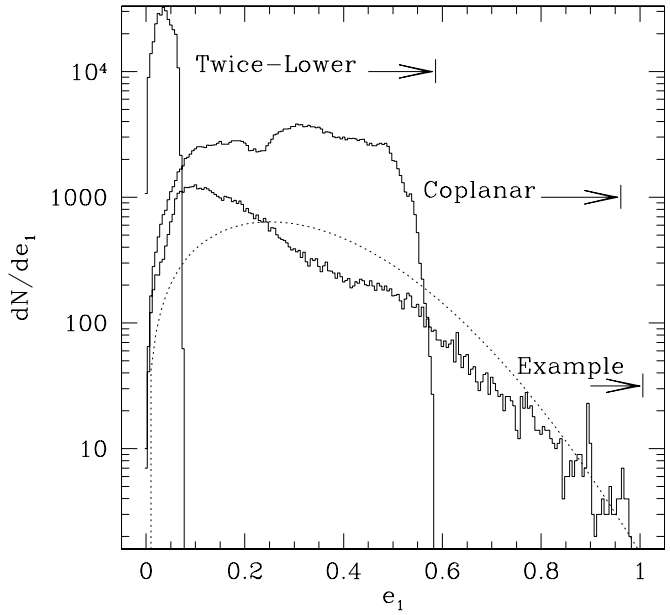

Figure 4. Probability distribution of the inner planet's eccentricity, dN/de_1, in the "example" system of Figure 1, in a system with twice-lower eccentricities and inclinations ("twice-lower"), and in a system that has the same eccentricities but is coplanar ("coplanar"). The first case is integrated for 300 Myr (stopped short when the planet reaches the zone of tidal circularization), while the latter two are integrated for 1.5 Gyr. The maximum eccentricity allowable in each case (see Figure 7) is marked by the arrows. Diffusion in the latter two cases is partially inhibited. The dashed line is a Rice distribution with mean 0.2 and variance 0.25. The example system is expected to approach the Rice distribution after a long time.

modes, and the spectral entropy rises toward $\ln 5$ over a 10^8 year timescale.

A third way to observe diffusion is to plot the probability distribution function of e_1, following Laskar (2008), as shown in Figure 4. For our example system, e_1 is broadly distributed from 0 to 1, with its distribution roughly described by a Rice function (Laskar 2008),

$$f(e) = \frac{e}{\sigma^2} \exp\left(\frac{-(e^2+\nu^2)}{2\sigma^2}\right) I_0\left(\frac{e\nu}{\sigma^2}\right), \qquad (11)$$

where I_0 is the modified Bessel function of the first kind with order 0. This is the expected distribution for $|z|$ if $z = x+iy$ with x and y being two independent Gaussian variables with mean ν and variance σ.

What is required for AMD diffusion to occur? We find that there must be a sufficient amount of AMD in the system. For instance, when integrating the example system, but with all secular mode amplitudes reduced by a factor of two (total AMD reduced to $1.17/4 = 0.29$, the "twice-lower" curve in Figure 4), or when flattening all orbits into coplanar ones (AMD = 0.72, the "coplanar" curve in Figure 4), we find that AMD diffusion is largely suppressed. While AMD allows e_1 to reach 0.58 ("twice-lower") and 0.955 ("coplanar"), diffusion is only able to bring e_1 to 0.15 and 0.58, respectively. Motion is either largely quasi-periodic or weakly chaotic. This is in contrast to the example case where the inner planet explores phase space and reaches its maximum eccentricities and inclinations.

Why does the amount of AMD make a difference? The interested readers are referred to Lithwick & Wu (2011) for detailed quantitative analysis. Here we only comment that to allow AMD diffusion, chaos is essential, and chaos is driven by the overlap of resonances (Chirikov 1979). The resonances of relevance are high order secular resonances. Their widths increase sharply with mode amplitude. A lowering of the mode amplitudes by a mere factor of two can shrink the resonance width by a large factor. This qualitatively explains why the twice-lower case is not chaotic. In a coplanar system, all resonances that involve the inclination modes are ineffective, and with fewer resonances to drive chaos, their dynamics become much more regular.

4.4. Chaotic Processes Leading to Hot Jupiters

Given the chaotic nature of the dynamics, the final state of the system depends sensitively on initial conditions. In our example case, we obtain a hot Jupiter with $a_1 = 0.027$ AU and an inclination of 70° at the end of the 300 Myr integration (Figure 2). In another case, modified from the previous one in energy and angular momentum by about 0.1% at time 293 Myr (just before the onset of tidal dissipation), we find that the inner planet narrowly avoids being tidally circularized into a hot Jupiter straightaway and is able to return its AMD to the outer planets. The eventual hot Jupiter thus formed has $a_1 = 0.04$ AU and an inclination of 25° (Figure 5). Our other experiments show that in some cases the tidal dissipation process is gradual and occurs over many episodes of high eccentricities. There could be an extended period during which the planet destined to become a hot Jupiter is temporarily parked at an intermediate distance (e.g., $a_1 = 0.1$ AU) with large eccentricities and inclinations. They may help to explain the presence of "warm Jupiters."

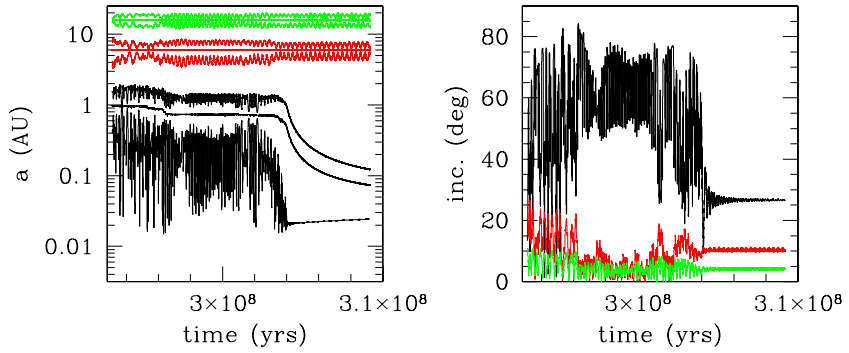

Figure 5. Evolution of a system that is slightly modified from that in Figure 2 by 0.1% in total orbital energy and angular momentum, at time $t = 2.93 \times 10^8$ yr. The subsequent trajectory differs. The inner planet in this case suffers some tidal dissipation at $t = 294$ Myr and migrates to $a_1 = 0.75$ AU. However, it avoids being turned into a hot Jupiter right away and returns its AMD to the outer planets (left panel). Secular chaos continues to operate until the inner planet is turned into a hot Jupiter with $a_1 = 0.04$ AU and an inclination of 25°. This demonstrates the sensitive dependence on initial conditions.

(A color version of this figure is available in the online journal.)

With a tidal quality factor for the planet of $Q_p = 10^5$, the example case sees most of the orbital binding energy deposited inside the planet within a couple Myr, with an averaged (over 1 Myr timescale) heating rate of 5×10^{29}erg s^{-1}, $\sim$15 times higher than the self-luminosity of a $T_{\rm eff} = 1000$ K Jovian planet. The total tidal energy deposited is $\sim 1.5 \times 10^{44}$erg, again about 15 times larger than the gravitational binding energy of the planet. This has the potential of disrupting the planet unless the heat is deposited into regions of short thermal time. However, if the tidal dissipation process is more gradual, the mode of heat deposition can be drastically different, potentially impacting the final sizes of hot Jupiters.

4.5. Effects of Mean-motion Resonances

MMRs, not to be confused with secular resonances, can also affect secular chaos. This is true even if the MMRs are of high order. Because MMRs can change the semimajor axes, the dynamical system has more degrees of freedom and can explore different parts of the phase space, potentially enhancing diffusion. We experiment by placing the outer two planets near the 2:1 MMR (6 AU and 9.52 AU). We find that diffusion proceeds quickly even with an AMD as low as 0.29, a value that corresponds to our twice-lower system (which shows regular behavior). But when we move the outer planet outward by a mere 0.5 AU, the system behaves regularly again. This confirms that, at least in this case, MMRs can be responsible for facilitating AMD equipartition.

In addition, even for systems which are not initially next to any lower order MMRs (such as our example case), as eccentricity and inclination rise to order-unity values, low order MMRs are activated. For the case shown in Figure 1, the semimajor axis of the inner planet undergoes increasingly large variations at late stages of the evolution,[9] perhaps indicating MMRs at work. Accompanying this is the non-conservation of AMD. Are MMRs a significant source of AMD? If so, they could allow the inner planet to reach a higher eccentricity than allowed by the initial AMD of the system. This intriguing possibility deserves to be explored.

Another possible connection between secular chaos and MMRs exists. In systems which are initially more compact than our example system, but not compact enough to have immediate close encounters, secular chaos increases the eccentricity of inner planets, allowing MMRs to function at later stages, leading finally to planet scattering well after the protoplanetary disks have dissipated.

5. PREDICTIONS FOR HOT JUPITERS

We have demonstrated that secular chaos can produce hot Jupiters. The remaining central issue is how prevalent this mechanism is. Is it prevalent enough to explain the observed frequency of hot Jupiters?

Unfortunately, since we do not know the initial configurations of planetary systems, it is difficult to predict the frequency of hot Jupiter production by secular chaos. We also face the problem that a systematic survey of the relevant parameter spaces is numerically expensive, at least using our current technique of N-body integration. So in the following, we discuss qualitative predictions based on our present understanding of secular chaos.

[9] The changes are on the percent level and are somewhat difficult to discern in that plot.

5.1. General Predictions

The predictions are ranked roughly in decreasing order of certainty.

1. A pile-up of hot Jupiters around 3 day orbital periods.

   The characteristic stalling at 3 day orbital periods that we observe in our simulations is explained by a combination of tidal precession and tidal dissipation (both due to tides on the planet). Precessions by other close-range forces (GR, rotational quadrupole) are less important. The tidal precession stalls the rise of the eccentricity to about a few times the Roche radii, and tidal dissipation finishes the job by circularizing the highly eccentric orbit to that of a hot Jupiter. The location of the pile-up remains largely unchanged even if the rate of tidal dissipation is orders of magnitude weaker. We stress that this prediction is not unique to secular chaos, but also applies to Kozai migration, or any other mechanism where eccentricity is slowly raised. By contrast, in planet scattering the eccentricity changes are sudden, and hence a 3 day pile-up would not be expected.
2. Hot Jupiters are lower in mass compared to other giant planets.

   This prediction stems from AMD conservation. To become a hot Jupiter, the inner planet has to reach an eccentricity so high that $a_1(1 - e_1) \leqslant 0.05$ AU. For a given amount of AMD, a lower mass inner planet can reach a higher eccentricity. Observationally, compared to giant planets at larger distances, there is a clear deficit of massive hot Jupiters (Zucker & Mazeh 2002; Udry & Santos 2007). If hot Jupiters migrated from the population to larger distances, the relevant migration mechanism would need to prefer low-mass planets. Kozai migration, in contrast, has no mass preferences (Wu et al. 2007).
3. Hot Jupiters have no companions within a few AU, but have companions roaming at larger distances.

   On the one hand, the high-eccentricity episode the inner planet undergoes before it is tidally captured implies that hot Jupiters have no companions within a few AU. This agrees with observations where hot Jupiters appear to be strikingly alone (Wright et al. 2009), and where attempts at measuring transit timing variations have repeatedly turned up empty-handed. On the other hand, secular chaos requires driving by other giant planets. They should be roaming at large distances (outside a few AU) and remain to be detected—some may have already shown up as RV residuals in hot Jupiter systems (Fischer et al. 2001; Wright et al. 2009). There is also the intriguing possibility that one of the companions is a binary star.
4. Frequency of hot Jupiters should rise with stellar age.

   Being a diffusive process, secular chaos operates on timescales comparable to or longer than the secular precession timescale. The latter, for our fiducial system, is of order $M_*/M_2 P_2^2/P_1 \sim 10^5$ yr. As such, we expect stars that are within a few tens of million years after their disk dispersal to have a lower hot Jupiter fraction than stars that are a few Gyr old. This prediction should be quantified by extensive numerical simulations that start with reasonably realistic planetary configurations.
5. Orbits of hot Jupiters could be strongly misaligned with stellar spin.

   We will discuss the planet inclination in Section 5.2.

If secular chaos is responsible for producing hot Jupiters, this has a number of implications for planetary systems at large.

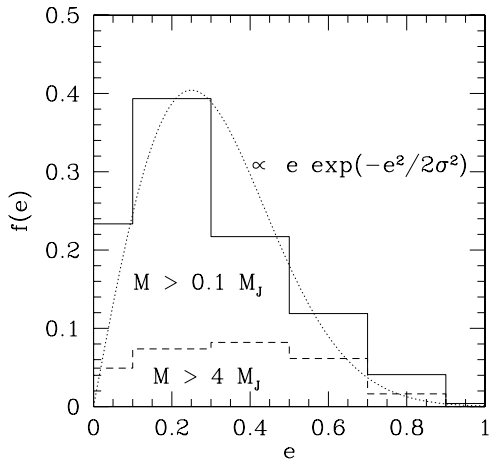

Figure 6. Eccentricity distribution of Jovian planets that have pericenter between 0.1 and 10 AU and projected masses above 0.1 M_J. (the solid histogram). The lower limit of 0.1 AU is selected to preclude planets that have undergone significant tidal circularization. The dotted line is the Rayleigh distribution with $\sigma = 0.25$. The sub-population of more massive planets with $M \sin i > 4\,M_J$ are represented by the dashed histogram. It appears that more massive planets have a hotter distribution.

1. A large number of planetary systems should have three or more giant planets on (mildly) eccentric, inclined orbits.

   Only systems that have sufficient AMD can make hot Jupiters. Hot Jupiters may be the tip of the iceberg in terms of their system AMD values. If so, then most giant planets we know of should reside in systems with three or more giant planets. There should still be residual AMD in the outer planets.

2. Warm Jupiters could arise from secular chaos and their orbits could be misaligned with respect to the stellar spin.

   We call giant planets at a few tenths of an AU "warm Jupiters," for the reason that they are at intermediate locations between hot Jupiters ($\sim 10^{-2}$ AU) and cold Jupiters (~a couple AU).

   Among those that fail to make hot Jupiters, there may be warm Jupiters—planets which have suffered some degree of tidal dissipation but have yet to be tidally captured into hot Jupiters. These planets are temporarily intercepted from their inward spiral by interactions with outer planets that can inject into their orbits a fresh boost of angular momentum. Eventually, these planets would be dragged in to become hot Jupiters, but while they are in their temporary parking space, their orbits could have high inclinations as well as high eccentricities. Observationally, there is a "period valley" at these distances, indicating that perhaps the warm Jupiter phase is relatively short lived. Measurements of spin–orbit angle for these planets will be useful constraints.

3. Even for systems where the inner planets cannot reach high enough eccentricity to be captured into hot Jupiters, secular chaos may have observable consequences.

   Starting from mildly eccentric, inclined orbits, inner planets in planetary systems may gradually extract AMD from outer planets. The long-term eccentricity and inclination distributions for these planets approach the Rice distribution (Figure 4). This reduces to a Rayleigh distribution when the centroid is much smaller than the variance. Figure 6 shows the observed eccentricity distribution of Jovian planets: it may be represented by a Rayleigh distribution with variance 0.25. If future R-M measurements provide us with a similar distribution for the orbital inclinations, this will be strong proof in favor of secular chaos.

   If secular chaos is largely responsible for the observed planet eccentricities, one expects that, for the same amount of AMD available in the system, lighter planets in general reach higher eccentricities. However, data (Figure 6) show an inverse correlation—more massive ($M \sin i > 4\,M_J$) planets have a hotter eccentricity distribution. This may be interpreted as being due to pollution from systems undergoing Kozai cycles induced by stellar companions, which are capable of exciting eccentricities even in very massive planets. This interpretation requires that massive planets occur preferentially in binary systems.

4. Secular chaos can stabilize planetary systems.

   In our simulation (Figure 1), the tidally captured hot Jupiter removes AMD from the system, stabilizing the outer planetary systems as a result. This could be a generic process in organizing planetary systems on long timescales.

5. Can secular chaos explain hot Neptunes or hot Earths?

   If the inner planet has a lower mass, it experiences a weaker near-range precession due to its smaller tidal and J2 moments. Equation (3) predicts that a Neptune-like planet ($M = M_N = 1/17\,M_J$ and $R = R_N = 0.36\,R_J$), driven to chaos by secular forcing of giant planets at a few AU, could be stalled at periapse distance ~0.009 AU, and hence it would be circularized at ~0.018 AU ~ $4\,R_\odot$. This distance would be approximately doubled if it is forced by other Neptune-mass planets, while a more inflated planet would also be stalled at a greater distance. Hot Neptunes thus produced will tend to have a broader pile-up than hot Jupiters, because the masses of the perturbers can extend over a large range. Such a mechanism could explain some of the observed hot Neptunes—for instance, the HD 125612 system where a hot Neptune is accompanied by two Jupiter-like planets at much larger distances (Lo Curto et al. 2010).

   Bouchy et al. (2009) noted that ~70% of low mass close-in planets (with $M \sin i < 0.1\,M_J$) have detected planetary companions. This differs from the hot Jupiter case. It likely relates to the lower requirement for the planetary spacing when the inner planet is less massive.

   An Earth-like planet, on the other hand, will not be stalled at large enough distances to avoid Roche lobe overflow. Secular chaos is an unlikely agent for making hot earths, especially considering that the tidal damping time for an Earth-like planet at 0.03 AU exceeds a Hubble time.

5.2. Stellar Obliquity

The final inclination of the inner planet deserves an in-depth discussion.

Fabrycky & Winn (2009) found that a majority of transiting planets have their orbits aligned with the stellar spin. However, that majority was quickly weakened by a slew of misaligned systems (Triaud et al. 2010). The current situation is best summarized in Morton & Johnson (2011), and a correlation between stellar obliquity and stellar spectral type has been noted (Winn et al. 2010).

Our example system (Figure 1) produces a hot Jupiter with an orbit inclined by 70° from the invariable plane of the planetary system, while its near-identical twin yields a hot Jupiter with an inclination of 25° (Figure 5). Secular chaos could in principle drive the inner planet to inclinations between 0° and 180° relative to the invariable plane (Figure 7), given the amount of AMD in this system. To demonstrate this, we turn off tidal

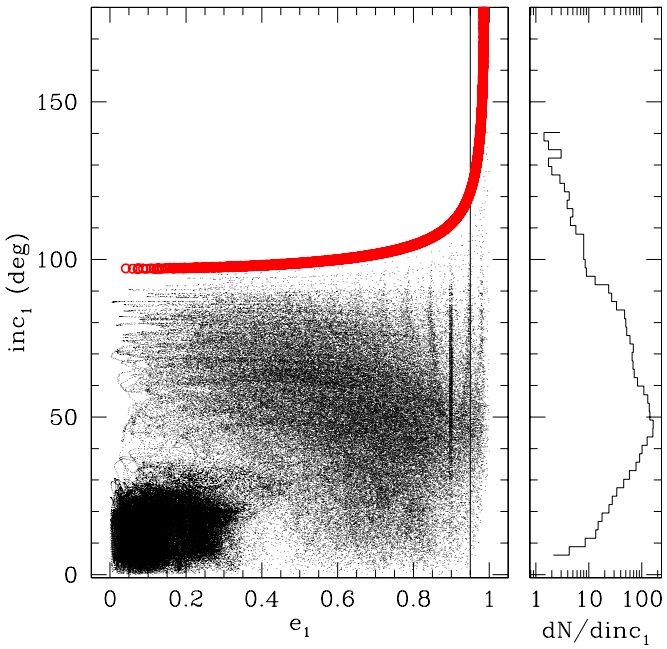

Figure 7. Eccentricity–inclination phase space that is traversed by the same system as Figure 1 over a total of 400 Myr, in the absence of tidal dissipation. The thick red curve bounds the region within which the inner planet can explore, as dictated by energy and angular momentum conservation (assuming constant a_i, so this is determined by the initial AMD). Secular chaos transports the inner planet to very high eccentricities (bounded at the right by near-range precessions) and to retrograde orbits. If tidal dissipation were turned on, it would operate rightward of the vertical line at $e = 0.95$ (pericenter distance of $a_1(1 - e_1) = 0.05$ AU). The right panel shows the distribution of inclinations whenever $e_1 > 0.95$. This can be regarded as an approximation to the distribution of final inclinations. For this system, retrograde orbits are achieved a few percent of the time.

(A color version of this figure is available in the online journal.)

dissipation in our example integration and evolve the fiducial system for 400 Myr. The eccentricity and inclination phase space traversed by the inner planet is presented in Figure 7. Within the constraint of AMD conservation, the planet is able to diffusively reach high eccentricity, with both prograde and retrograde orbits. The final inclination for the hot Jupiter then depends on chance.

In Figure 7, we also display the distribution of inclinations whenever $1 - e_1 \leqslant 0.05$, as a proxy for the final inclinations of hot Jupiters. We find that retrograde orbits represent a few percent of the total for a given value of the AMD in the system. The preponderance of prograde orbits is related to the prograde initial condition.

This result is specific to our example system and is relative to the invariable plane. The invariable plane does not necessarily coincide with the stellar equatorial plane—the relative angle is only 7° in the solar system, but it can be large elsewhere.[10]

6. SUMMARY

Hot Jupiters, while representing only a small fraction of all known extra-solar planets, demand special attention. They are most at odds with planet formation theory; they are detected disproportionately in RV and transit surveys; and they are most accessible to characterization. Their rarity may indicate that their formation requires extreme circumstances. However, they may teach us much about the general conditions of planetary systems.

Hot Jupiters are piled up around 3 day orbital periods, with rapid cutoffs both inward and outward of this distance; they tend to be less massive than more distant planets; many of them have orbits that are misaligned relative to the stellar spin; and they are remarkably anti-social as they have few detected companions.

In this work, we show that most of these characteristics can be explained if hot Jupiters are produced by secular chaos. These planets, originally located at $\gtrsim$1 AU, acquire AMD from planets that are farther out in the system. The outer planets can be mildly eccentric and/or inclined, but the same AMD produces much greater eccentricities and inclinations when it is transported to an inner planet, especially if the inner planet is less massive than the outer ones. The extremely high eccentricity allows the inner planet to reach inward of a few stellar radii and be tidally ensnared by the central star into a hot Jupiter.[11] We find that the criterion for hot Jupiter production is a sufficient amount of AMD.

Only five hot Jupiters have known planetary companions, and these companions are typically eccentric and may have contributed to secular chaos. We note that the hot Jupiter (at 0.06 AU) in the Ups And system, where two other massive planets orbit at 0.8 and 2.5 AU, with eccentricities of 0.2 and 0.3, respectively, may well be produced by the secular chaos presented here.[12] This possibility is further boosted by the recent finding that the two outer planets' inclinations are misaligned by ∼30° from each other (McArthur et al. 2010). Similarly, the retrograde hot Jupiter in WASP-8b (Queloz et al. 2011) is in a stellar system including an M-star companion at ∼600 AU. Moreover, the RV trend indicates a companion at distance >1 AU that is more massive than $2\,M_J$. This could also be a hot Jupiter produced by secular chaos, with the M-star acting as the third planet.

Hot Neptunes may also be formed via secular migration. However, hot Earths are different. It is not that Earth-like planets could not undergo secular chaos, but that once they do, they cannot be stalled at a safe enough distance to avoid being swallowed by the central star.

Secular chaos has also been found to be responsible for instability in the inner solar system (Laskar 2008; Lithwick & Wu 2011). We speculate that secular chaos may be a frequent phenomenon in planetary systems. It may help to excite inner planets to higher eccentricities or inclinations. If these planets are removed, the remaining planetary systems may be stabilized for a time comparable to the system age.

The success of this theory depends on two unknown factors. One is the amount of initial AMD in the system. The other is the typical configuration of planetary systems when emerging out of the protoplanetary disk. It also needs to be demonstrated solidly that secular chaos can lead to a large fraction of retrograde hot Jupiters. Observationally, if not only hot planets but also warm or cold planets can be shown to have significant orbital inclinations relative to the spin of their host stars, this would boost the case for the ubiquity of secular chaos. Future R-M

[10] Here, we have assumed that the stellar spin is aligned with the invariable normal when calculating precession due to the stellar rotational bulge.

[11] Kozai migration is another process that may give rise to large eccentricity to Jovian planets. Such planets may be similarly captured into hot Jupiters. Since Kozai oscillation is also a secular forcing, we propose to name both secular chaos and Kozai migration generically as "secular migration."

[12] The companions are detectable in this case because this is a scaled-down version of the systems we investigated. The inner planet may initially be at $a \sim 0.2$ AU, as opposed to $a = 1$ AU as in Figure 1.

measurements should be extended to transiting planets at large distances.

We thank Peter Goldreich, Jeremy Goodman, Norm Murray, Daniel Fabrycky, Scott Tremaine, Eiichiro Kokubo, and Doug Lin for discussions. We both enjoyed the hospitality of KIAA Beijing where part of this work was performed. We thank the referee, Makiko Nagasawa, for helpful suggestions. Y.W. further acknowledges the NSERC funding and a Caltech sabbatical stay. Lastly, we thank M. Duncan and H. Levison for the use of their SWIFT package.

APPENDIX

The standard SWIFT package distribution does not contain a treatment for the GR precession, or precession due to tidal and rotational bulges. These dominate over secular precession by other planets when the inner planet reaches very close to the host star. Together with tidal dissipation, these effects determine the final orbit of the planet, as well as the timescale for tidal circularization. Below is our implementation of all these processes in the SWIFT code. Since non-Keplerian accelerations in the symplectic SWIFT integrator are incorporated as velocity kicks between Keplerian drifts, we need expressions for the perturbative accelerations.

To first order in $(v/c)^2$, the GR effect can be written as a perturbation to the Newtonian gravitational potential as

$$\Phi_{\rm GR} = -\frac{GM_* L^2}{c^2 m_p^2 r^3}, \tag{A1}$$

where r is the radial distance between the star and the planet, and $L = m_p\sqrt{GM_* a(1-e^2)}$ is the orbital angular momentum. The purely radial force associated with this potential,

$$\mathbf{a}_{\rm GR} = -\boldsymbol{\nabla}\Phi_{\rm GR} = -\frac{3G^2 M_*^2 a(1-e^2)}{c^2 r^4}\,\hat{\mathbf{r}}, \tag{A2}$$

gives rise to a precession of the eccentricity vector. We confirm that such a numerical procedure yields the following orbit-averaged precession rate for the longitude of the pericenter (Einstein 1916)

$$\dot{\varpi}_{\rm GR} = \frac{3GM_* n}{c^2 a(1-e^2)}. \tag{A3}$$

For the tidal effects, we first consider the rotational bulge and the tidal bulge on the star. The following expressions are from Sterne (1939), differing only in notation. Let the stellar spin rate be ω_*, radius R_*. The centrifugal potential due to the stellar spin, and the quadrupole tidal potential due to the planet acting on a point at distance $\mathbf{D}$ away from the stellar center, is

$$\Phi_{\rm acting} = +\frac{1}{3}\omega_*^2 D^2 P_2(\cos\theta') - \frac{Gm_p}{r}\left(\frac{D}{r}\right)^2 P_2(\cos\theta). \tag{A4}$$

Here, the Legendre function $P_2(x) = 1/2\,(3x^2-1)$, and the connecting angles are defined as $\cos\theta = \hat{\mathbf{D}}\cdot\hat{\mathbf{r}}$, $\cos\theta' = \hat{\mathbf{D}}\cdot\hat{\omega}_*$, where $\mathbf{r}$ is the vector connecting the two bodies. The global distortion of the star under the above potential casts a response potential in its surrounding (measured at position $\mathbf{D}$)

$$\Phi_{\rm reponse} = \frac{k_{2*}R_*^5}{D^3}\left[\frac{\omega_*^2}{3}P_2(\cos\theta') - \frac{Gm_p}{r^3}P_2(\cos\theta)\right], \tag{A5}$$

where k_2 is the Love number and is taken to be 0.029 for the star (polytrope $n = 3$) and 0.52 for the planet (polytrope $n = 1$).[13] The barycentric acceleration that the reduced particle feels is therefore

$$\mathbf{a} = -\frac{m_p}{\mu}\boldsymbol{\nabla}\Phi_{\rm response}, \tag{A6}$$

where the reduced mass $\mu = m_* m_p/(m_* + m_p)$.

We trace the planetary motion in the frame of the invariable plane and we assume that the stellar spin coincides with the normal of the invariable plane. So, at the heliocentric position of the planet (x, y, z), $\cos\theta = 1$ and $\cos\theta' = z^2/r^2$, where $r^2 = x^2 + y^2 + z^2$. Here, the z^2 term in the potential gives rise to spin–orbit coupling and the orbit normal of the planet precesses around the spin direction.

The bulges on the planet are treated similarly, except we assume that the planet spin is aligned with the orbit normal, so $\cos\theta' = 0$.

The above close-range accelerations are expressed for the barycentric movement. However, one should correct for the fact that the kick asked by the SWIFT code is the heliocentric value.

The dissipative part of the tidal effect is handled in a way that differs from the standard treatment of Lee & Peale (2003). We use the weak friction prescription for the equilibrium tidal bulge, and calculate the effect of dissipation in both the star and the planet. The tidal bulge raised on either body produces a potential given by the second term in Equation (A5). Due to finite dissipation inside the body, there is a delay between the response and the forcing. We can assume either a constant time lag (τ) or a constant phase lag (ϵ). In the latter case, we can introduce a tidal Q factor (Goldreich & Soter 1966), which is related to the phase lag and the time lag as $\epsilon = 1/Q$ and $\tau = \frac{1}{Q}\frac{2\pi}{\omega_{\rm tide}}$, respectively. Here, $\omega_{\rm tide}$ is the tidal forcing frequency. For the eccentricity tide, $\omega_{\rm tide}$ is simply $2n$. The acceleration associated with the delayed tidal bulge raised on body M (with radius R) by body m at distance r is (Hut 1981)

$$-\frac{Gm^2}{\mu r^2}\left(\frac{R}{r}\right)^5 k_2\left[\left(3 + 9\frac{\dot{r}}{r}\tau\right)\hat{\mathbf{r}} - (\omega - \dot{\theta})\tau\hat{\theta}\right], \tag{A7}$$

where ω is the rotational velocity and $\dot{\theta}$ the instantaneous orbital angular velocity. In particular, $\dot{r} = nae\sin f/\sqrt{1-e^2}$ for a Keplerian ellipse. The first half of the radial term contributes to orbital precession (dealt with above) but no energy dissipation (as it is anti-symmetric within a Keplerian ellipse and cancels out over an orbit). We ignore the angular force that transfers angular momentum—the spin angular momentum of the planet is much smaller than its orbital angular momentum and so we assume that the planet is quickly synchronized with the orbit, while we assume that the tidal Q factor associated with the star is so large that there is no angular momentum being transported between the orbit and the stellar spin. So, we are left with only the second half of the radial force. This is easily implemented in the SWIFT package. We adopt values of $Q_p = 10^5$ and $Q_* = 10^{10}$ for our work. Thus, tidal dissipation is dominated by that inside the planet.

REFERENCES

Agol, E., Steffen, J., Sari, R., & Clarkson, W. 2005, MNRAS, 359, 567
Batygin, K., & Laughlin, G. 2008, ApJ, 683, 1207

[13] It is larger than the apsidal motion constant in binary studies (also written as k_2) by a factor of two.

Bouchy, F., et al. 2009, A&A, 496, 527
Butler, R. P., et al. 2006, ApJ, 646, 505
Chambers, J. E. 2009, Annu. Rev. Earth Planet. Sci., 37, 321
Chatterjee, S., Ford, E. B., Matsumura, S., & Rasio, F. A. 2008, ApJ, 686, 580
Chirikov, B. V. 1979, Phys. Rep., 52, 263
Csizmadia, S., et al. 2010, A&A, 510, A94
Cumming, A., Butler, R. P., Marcy, G. W., Vogt, S. S., Wright, J. T., & Fischer, D. A. 2008, PASP, 120, 531
Eggleton, P. P., & Kiseleva-Eggleton, L. 2001, ApJ, 562, 1012
Einstein, A. 1916, Ann. Phys., Lpz., 354, 769
Fabrycky, D., & Tremaine, S. 2007, ApJ, 669, 1298
Fabrycky, D. C., & Winn, J. N. 2009, ApJ, 696, 1230
Fischer, D. A., Marcy, G. W., Butler, R. P., Vogt, S. S., Frink, S., & Apps, K. 2001, ApJ, 551, 1107
Ford, E. B., Havlickova, M., & Rasio, F. A. 2001, Icarus, 150, 303
Ford, E. B., & Rasio, F. A. 2006, ApJ, 638, L45
Ford, E. B., & Rasio, F. A. 2008, ApJ, 686, 621
Fressin, F., Guillot, T., Morello, V., & Pont, F. 2007, A&A, 475, 729
Fukui, A., et al. 2011, PASJ, 63, 287
Gaudi, B. S., Seager, S., & Mallen-Ornelas, G. 2005, ApJ, 623, 472
Goedde, C. G., Lichtenberg, A. J., & Lieberman, M. A. 1992, Phys. D Nonlinear Phenom., 59, 200
Goldreich, P., & Soter, S. 1966, Icarus, 5, 375
Hebrard, G., et al. 2010a, A&A, 513, 69
Hebrard, G., et al. 2010b, A&A, 516, 95
Herbst, W., & Mundt, R. 2005, ApJ, 633, 967
Holman, M. J., & Murray, N. W. 2005, Science, 307, 1288
Hrudková, M., et al. 2010, MNRAS, 403, 2111
Hut, P. 1981, A&A, 99, 126
Jurić, M., & Tremaine, S. 2008, ApJ, 686, 603
Kozai, Y. 1962, AJ, 67, 591
Lai, D., Foucart, F., & Lin, D. N. C. 2011, MNRAS, 412, 279
Laskar, J. 1989, Nature, 338, 237
Laskar, J. 1997, A&A, 317, L75
Laskar, J. 2008, Icarus, 196, 1
Laskar, J., & Gastineau, M. 2009, Nature, 459, 817
Laughlin, G., Deming, D., Langton, J., Kasen, D., Vogt, S., Butler, P., Rivera, E., & Meschiari, S. 2009, Nature, 457, 562
Lee, M. H., & Peale, S. J. 2003, ApJ, 592, 1201
Levison, H. F., & Duncan, M. J. 1994, Icarus, 108, 18
Libert, A.-S., & Henrard, J. 2005, Celest. Mech. Dyn. Astron., 93, 187
Lin, D. N. C., Bodenheimer, P., & Richardson, D. C. 1996, Nature, 380, 606
Lin, D. N. C., & Papaloizou, J. 1986, ApJ, 309, 846
Lithwick, Y., & Wu, Y. 2011, arXiv:1012.3706
Livi, R., Pettini, M., Ruffo, S., Sparpaglione, M., & Vulpiani, A. 1985, Phys. Rev. A, 31, 1039
Lo Curto, G., et al. 2010, A&A, 512, A48
Maciejewski, G., et al. 2010, MNRAS, 407, 2625
Maciejewski, G., et al. 2011, MNRAS, 411, 1204
Marcy, G., Butler, R. P., Fischer, D., Vogt, S., Wright, J. T., Tinney, C. G., & Jones, H. R. A. 2005, Prog. Theor. Phys. Suppl, 158, 24
Matsumura, S., Thommes, E. W., Chatterjee, S., & Rasio, F. A. 2010, ApJ, 714, 194
McArthur, B. E., Benedict, G. F., Barnes, R., Martioli, E., Korzennik, S., Nelan, E., & Butler, R. P. 2010, ApJ, 715, 1203
Michtchenko, T. A., Ferraz-Mello, S., & Beaugé, C. 2006, Icarus, 181, 555
Michtchenko, T. A., & Malhotra, R. 2004, Icarus, 168, 237
Migaszewski, C., & Goździewski, K. 2009, MNRAS, 395, 1777
Milankovitch, M. 1941, Kanon der Erdbestrahlungen und seine Anwendung auf das Eiszeitenproblem (Belgrade: Königlich Serbischen Akademie)
Morton, T. D., & Johnson, J. A. 2011, ApJ, 729, 138
Murray, C. D., & Dermott, S. F. 2000, Solar System Dynamics (Cambridge: Cambridge Univ. Press)
Naef, D., et al. 2001, A&A, 375, L27
Nagasawa, M., Ida, S., & Bessho, T. 2008, ApJ, 678, 498
Naoz, S., Farr, W. M., Lithwick, Y., Rasio, F. A., & Teyssandier, J. 2011, Nature, 473, 187
Papaloizou, J. C. B., & Terquem, C. 2001, MNRAS, 325, 221
Pätzold, M., & Rauer, H. 2002, ApJ, 568, L117
Pont, F., et al. 2009, A&A, 502, 695
Queloz, D., et al. 2011, A&A, 517, 1
Rabus, M., Deeg, H. J., Alonso, R., Belmonte, J. A., & Almenara, J. M. 2009, A&A, 508, 1011
Rasio, F. A., & Ford, E. B. 1996, Science, 274, 954
Raymond, S. N., Barnes, R., Veras, D., Armitage, P. J., Gorelick, N., & Greenberg, R. 2009, ApJ, 696, L98
Rice, W. K. M., Armitage, P. J., & Hogg, D. F. 2008, MNRAS, 384, 1242
Shakura, N. I. 1985, Pis ma Astron. Zh., 11, 536
Sidlichovsky, M. 1990, Celest. Mech. Dyn. Astron., 49, 177
Sterne, T. E. 1939, MNRAS, 99, 451
Triaud, A. H., et al. 2010, A&A, 524, 25
Udry, S., Mayor, M., & Santos, N. C. 2003, A&A, 407, 369
Udry, S., & Santos, N. C. 2007, ARA&A, 45, 397
Winn, J. N., Fabrycky, D., Albrecht, S., & Johnson, J. A. 2010, ApJ, 718, 145
Winn, J. N., et al. 2005, ApJ, 631, 1215
Winn, J. N., et al. 2009, ApJ, 703, 2091
Wittenmyer, R. A., O'Toole, S. J., Jones, H. R. A., Tinney, C. G., Butler, R. P., Carter, B. D., & Bailey, J. 2010, ApJ, 722, 1854
Wright, J. T., Upadhyay, S., Marcy, G. W., Fischer, D. A., Ford, E. B., & Johnson, J. A. 2009, ApJ, 693, 1084
Wu, Y., & Goldreich, P. 2002, ApJ, 564, 1024
Wu, Y., & Murray, N. 2003, ApJ, 589, 605
Wu, Y., Murray, N. W., & Ramsahai, J. M. 2007, ApJ, 670, 820
Zucker, S., & Mazeh, T. 2002, ApJ, 568, L113